Evolution of Composition, Molar Mass, and Conductivity during the Free Radical Copolymerization of Polyelectrolytes†

Alina M. Alb,‡ Ahmet Paril,§ Huceste Çatalgil-Giz,§ Ahmet Giz,§ and Wayne F. Reed*,‡

Physics Department, Tulane University, New Orleans, Louisiana 70118, and Istanbul Technical University, 80626 Maslak, Istanbul

Received: December 21, 2006; In Final Form: March 7, 2007

Despite their importance in biological and technological contexts, copolymeric polyelectrolytes (or "copolyelectrolytes") continue to present challenges to theorists and experimentalists. The first results of a unified approach to the kinetics and mechanisms of copolyelectrolyte synthesis and the physical characteristics of the resulting polymers are presented. The free radical copolymerization of 4-vinylbenzenesulfonic acid sodium salt and acrylamide was monitored using automatic continuous online monitoring of polymerization reactions (ACOMP), from which the average bivariate composition and mass distributions were determined. Composition drift was related to the evolution of conductivity. In some cases bimodal populations of copolyelectrolyte and homopolymeric poly(acrylamide) resulted, i.e., blends of copolyelectrolyte and neutral homopolymer. The end-product scattering behavior depended on whether the end-product was bimodal or not, as demonstrated using automatic continuous mixing (ACM) in conjunction with light scattering and viscosity. Negative light-scattering third virial coefficients were found for bimodal end-products. This combined approach may allow connecting the synthesis kinetics to the resulting "trivariate" distribution of composition, molar mass, and linear charge density, which in turn controls the properties of end-product solutions, such as chain conformations, interparticle interactions, viscosity, interactions with colloids and other polymers, phase separation, etc. Unified results may allow testing and improvement of existing polyelectrolyte theories, development of new quantitative physicochemical models, provide advanced characterization methods, set the stage for studying more complex copolyelectrolytes, such as hydrophobically modified ones, and provide tools for ultimately controlling and tailoring the synthesis and properties of copolyelectrolytes.

Introduction

In this work new analytical tools allow a unified approach to understanding copolyelectrolytes. Copolyelectrolytes combine the functional characteristics of copolymers with the unusual properties of polyelectrolytes. Copolyelectrolytes are copolymers in which at least one of the comonomers is electrically charged.

Post-polymerization analysis for determining the copolymer bivariate mass/composition distribution currently relies on complicated, tedious cross-fractionation and other coupled techniques. These include calorimetry and densimetry,[1] liquid chromatography,[2] temperature rising elution fractionation,[3−6] crystallization analysis fractionation,[7] and techniques involving multidetector SEC alone,[8,9] SEC/NMR,[10] SEC/MALDI,[11] and SEC/thin layer chromatography.[12,13] Chromatographic techniques for composition analysis were recently reviewed.[14]

Long-range electrostatic forces are preeminent in polyelectrolytes. At very low ionic strength (IS), there are strong interparticle correlations that lead to angular scattering peaks of neutrons,[15−17] X-rays,[18] and light,[19−22] including under shear.[23] The ability to screen these effects with ionic strength (IS), leads to dramatic changes in polyelectrolyte properties. As IS increases, electrostatic excluded volume (EEV) and electrostatic persistence lengths (EPL) decrease, the strong interparticle correlations disappear, the polyelectrolyte coil shrinks, and light scattering increases while intrinsic viscosity decreases. A number of theories have been successful in grouping and unifying these phenomena.[24,−27]

It is well-known experimentally that the effective charge of a polyelectrolyte as measured by conductivity, electrophoresis,[28−31] and other means is often less than its chemical or stoichiometric charge. This is related to counterion condensation (CC),[32,33] for which a strong literature in analytical and numerical[34,35] theory and simulations abounds, but for which far fewer detailed experimental works exist.[36,37] In its simplest form,[73] the theory predicts that when the linear charge density, ξ (where ξ represents the number of elementary charges per Bjerrum length), of a long, rigid, polyelectrolyte rod exceeds one elementary charge (e) per Bjerrum length l_B ($l_B = 0.71$ nm in water at 25 °C), counterions will condense onto the polyelectrolyte until there is one e per l_B. More powerful approaches, taking into account factors such as chain flexibility and total free energy, counterion entropies, nonlinear Poisson−Boltzmann equation, ion correlations, and other effects, predict that the condensation phenomena are much richer and subject to many more factors than the naive theory predicts.[38−40]

Automatic continuous online monitoring of polymerization reactions (ACOMP) was introduced in 1998,[41] and provides a means of following the evolution of the average composition and molar mass distributions during the reaction. It is a nonchromatographic technique that requires the continuous

† Part of the special issue "International Symposium on Polyelectrolytes (2006)".

* Corresponding author. E-mail: wreed@tulane.edu. Phone: 504-862-3185. Fax: 504-862-8702.

‡ Tulane University.

§ Istanbul Technical University.

10.1021/jp0688299 CCC: $37.00
Published on Web 04/19/2007

TABLE 1: Combined ACOMP/ACM Results for VB/AaM Copolymers[a]

expt. #	1	2	3	4	5	6
VB% (M)	0	10	25	50	75	100
d*n*/d*c* (cm^3/g)	0.163	0.148	0.157	0.173	0.172	0.171
A_3 (cm^6 mol g^{-3})	0.0073	−0.0974	−0.2442	1.0455	1.1027	1.0853
A_2 (cm^3 mol g^{-2})	4.69×10^{-4}	1.90×10^{-4}	4.89×10^{-4}	5.78×10^{-4}	3.23×10^{-4}	2.71×10^{-4}
$[\eta]_{w,ACM\ 0.010M\ NaCl}$	130	122	184	333	393	440
$[\eta]_{w,ACM\ 0.3M\ NaCl}$	128	70	60	95	127	140
$M_{w,SEC}$	459 000	NA	179 000	309 000	425 000	702 000

[a] $C_{m0,reactor} = 0.3636$ M, 0.100 M NaCl in reactor and ACOMP detectors. ACM experiments listed here were done in 0.010M NaCl solutions. SEC solvent: 0.100 M NH_4NO_3+0.2 g/L NaN_3.

withdrawal of a small sample stream from the reactor, which is diluted to the degree that measurements made on the flowing sample are dominated by single particle properties, not by polymer interactions. Typically, combining multiangle light scattering, ultraviolet absorption, viscometry, and differential refractometry allows the determination of comonomer conversion, composition drift, and average composition and molecular mass distributions. It has been successfully applied to free radical and controlled free radical gradient copolymerization.[42,43]

It is interesting to compare ACOMP with in situ methods such as NIR and Raman. While ACOMP gives the comonomer conversions, which those techniques also do, ACOMP additionally monitors the evolution of weight average molar mass M_w and weight average intrinsic viscosity, $[\eta]_w$. An advantage of Raman and NIR compared to ACOMP is that probes for the former can often be put inside the reactor, avoiding ACOMP's complex withdrawal, dilution, and conditioning steps. The in situ probes also eliminate the delay times inherent to ACOMP. On the other hand, whether a probe is inserted into a reactor or a tube for withdrawal is inserted for ACOMP, access into the reactor is required in either case, and hence all techniques are "invasive" to this degree. Furthermore, probes inside of reactors can easily foul and lead to erroneous data. Working at high concentrations in the reactor normally requires that empirical models and calibrations be used to interpret in situ data.[44] In fact, calibration difficulties with Raman are well-known, and whole articles are devoted to them.[45] In contrast, the "front-end" (extraction, dilution, and conditioning, such as filtration, debubbling, phase inversion, etc.) of ACOMP is a flexible platform and specifically designed to deal with the conversion of real, often nonideal reactor contents into a highly conditioned, dilute, and continuous sample stream on which absolute, model-independent measurements can be made.

The current work characterizes the origins of some copolyelectrolyte properties, by combining recent advances in ACOMP with polyelectrolyte equilibrium characterization using automatic continuous mixing (ACM). The main thrust is to follow the effects of the kinetics of synthesis on the characteristic distributions and the effects of these distributions on the solution properties of the final copolyelectrolyte end-product. While the experimental trail is set out in this work connecting synthesis with some end-product solution behavior, a full theoretical unification will require considerable work.

Experimental Methods

Acrylamide (Aam) and 4-vinylbenzenesulfonic acid sodium salt (VB) were obtained from Fluka. Copolymerizations were initiated in aqueous solution at 60 °C, with 2,2′-Azobis(2-amidinopropane)dihydrochloride (V50). Different values of IS in the reactor were used for different reactions, although the majority of results presented here were carried out in 0.100M NaCl in the reactor. A total monomeric concentration, the sum of VB and Aam, of 0.364M was used in all experiments.

The ACOMP procedure involved continuous withdrawal of a small stream of reactor solution (0.1 mL/min), with a 2% dilution in the first dilution stage in a low-pressure mixing chamber, followed by different ratios of dilution in the second stage, in a high pressure mixing chamber, to produce a total solute concentration of ~0.4 mg/mL in the detector train). Each dilution stage was made with in 0.100 M NaCl aqueous solvent. The detector train included a dual wavelength UV spectrophotometer (a Shimadzu AV-10vp operating at 206 and 260 nm), custom-built capillary viscometer, Waters 410 refractive index detector (RI), and a custom built multi-angle light scattering unit. A conductivity probe (YSI 32, Yellow Springs Instruments Co., Inc.) was inserted in the reactor, and its signals captured with those from the other instruments via an Analog Digital converter.

The polyelectrolyte properties of the evolving copolymer could be enhanced by using a lower IS in the ACOMP diluent, i.e., using lower IS leads to more pronounced changes in light scattering and viscosity due to less suppression of electrostatic effects. This is not pursued here. It is emphasized, however, that all experiments in ACM and ACOMP use high enough IS for detection that polyelectrolyte effects commonly observed at very low IS are not manifest, i.e., the electroviscous effect and angular scattering maxima, which in dilute solutions normally are observed below IS of 0.001 M.

Table 1 shows the different starting ratios of VB and Aam (expressed as mol/mol in %/%) for each experiment, and the numbering scheme. Also shown is the value of dn/dc measured for each reaction end-product at constant IS. It has been known for many decades that formally one should use d*n*/d*c* determined in osmotic pressure equilibrium (such as results from "dialysis equilibrium").[46−48] While this is true in theory, a perusal of the literature reveals that authors have often introduced more experimental error into the d*n*/d*c* determination, e.g., from the swelling of dialysis membranes and consequent uncertainty in polymer concentration, leakage of low molar mass polymer into the dialysate, etc., than they are theoretically correcting for by trying to measure d*n*/d*c* at constant osmotic pressure. Literature values for osmotic equilibrium d*n*/d*c* can vary by over 30%.[49]

Automatic continuous mixing (ACM)[50] was used to characterize reaction end-products by alternately ramping polymer concentration at fixed IS, or vice versa.

Results and Discussion

Figure 1 shows raw data for a 10/90 (%) ([VB]/[Aam]) copolymerization reaction in aqueous 0.0002 M NaCl and 0.364 M total comonomer. After solvent baseline stabilization, Aam was added, and the UV_{206} nm signal increased. With subsequent addition of VB, both UV signals and conductivity σ, increased. The UV extinction coefficients for Aam and VB were determined from the UV detector response to their stepwise additions, and used subsequently to compute the concentration of each comonomer during the reaction by solving the two simultaneous

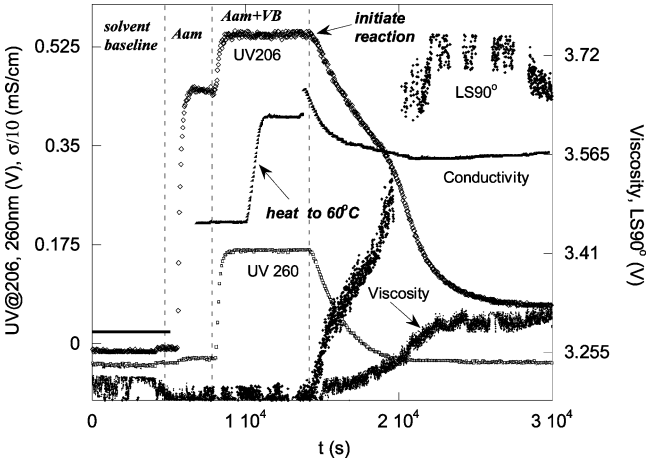

Figure 1. Raw ACOMP data for 10/90 ([VB]/[Aam]) copolymerization in 0.0002 M NaCl.

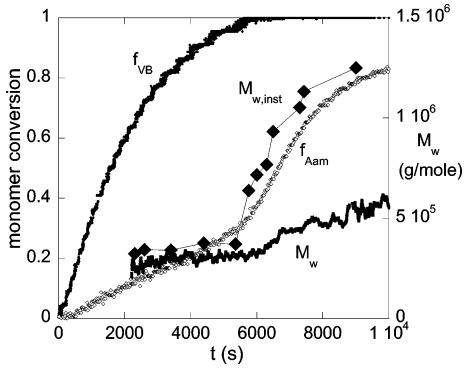

Figure 2. Comonomer conversions f_{VB}, f_{Aam}, and cumulative and instantaneous weight-averaged masses, M_w, and $M_{w,inst}$, respectively, for experiment #2 (not Figure 1 data).

equations from the dual wavelength UV data. The 260 nm signal is dominated by VB absorption, whereas the 206 nm signal is dominated by Aam absorption. Hence, when regarding Figure 1, to a first approximation the decrease of the 206 and 260 nm signals serve as visual guides to Aam and VB conversion, respectively.

When the reactor temperature reached 60 °C, initiator was added (15 000 s). VB was copolymerized faster than Aam in first-order fashion during the first phase of the reaction, seen by the 260 nm signal. After VB was exhausted, the remaining Aam homopolymerized rapidly; both phases can be seen in the 206 nm signal. Hence, inadvertently, a blend of copolyelectrolyte and PAM homopolymer was produced. σ decreased as VB was incorporated into copolyelectrolyte in the first phase, and remained constant in the second phase of Aam homopolymerization.

Figure 2 shows the fractional conversion of each comonomer, f_{VB} and f_{Aam}, respectively, for the same reaction in 0.100 M NaCl, obtained from the dual wavelength UV data. The two-phase behavior of f_{Aam} is striking. Its polymerization rate increases when the VB is exhausted.

The figure also shows the cumulative weight average mass M_w, which is seen to rise after the VB conversion phase is complete. The instantaneous M_w is also shown in Figure 2, and indicates that during the initial copolymerization phase a constant 3.5×10^5g/mol copolymer is produced, whereas $M_{w,inst}$ jumps dramatically to over 10^6 g/mol during the second phase of PAM homopolymer production. $M_{w,inst}$ is obtained from the cumulative M_w by[51]

$$M_{w,inst} = \frac{d\{fM_w(f)\}}{df} \quad (1)$$

The average composition drift can be followed in terms of the mole fraction of VB incorporated into copolyelectrolyte formed at any instant, $Z_{inst,VB}$, given by

$$Z_{inst,VB} = \frac{d[VB]}{d([VB] + [Aam])} \quad (2)$$

This is shown in Figure 3. VB comprises nearly 50% of early chains, and drops to 0% by 42% total comonomer conversion, as can be computed from the f_{VB} and f_{Aam} data in Figure 2. The average composition distribution, $df/dZ_{inst,VB}$, is then computed from $Z_{inst,VB}$,[43] shown in the inset; an essentially equal distribution of chains containing 47% VB and less are produced. The high rectangular region represents the amount of pure PAM homopolymer, produced in the last 58% conversion.

A starting hypothesis concerning the ξ distribution is that the evolution of σ, such as that in Figure 1, is related to the evolution of ξ, and a means to connect them must be found. Given the number of factors that influence σ in polyelectrolyte solutions, however, it is beyond the scope of this work to make a definitive determination of the ξ distribution. Initial trends can nonetheless be discerned.

During reactions, σ decreases, as charged monomers are linked into copolymer chains. When CC occurs, however, σ will decrease more per charged monomer linked than without CC, since both a charged monomer and its "condensed counterion" no longer contribute to σ. Hence, changes in the derivative of σ with respect to the charged monomer concentration can signal changes in fractional ionization of incorporated charged monomers, although the quantitative relationship is not simple. This may occur, e.g., if a highly reactive charged monomer is quickly incorporated into a copolymer with a neutral comonomer early in a reaction, producing chains above the CC threshold, but as the charged monomer is depleted ξ may drop below the CC, and hence begin to track the composition distribution.

The high initial slope of σ versus f_{VB} in Figure 3 suggests significant CC early in the reaction. The average spacing between VB monomers on the chain is $\ell = d/Z_{inst,VB}$, where d is the monomer contour length, ~0.26 nm. A dimensionless length scale ℓ/ℓ_B gives the average number of ℓ_B between VB monomers. For $\ell/\ell_B < 1$, when CC is expected, $Z_{inst,VB} > 0.36$. Hence, in Figure 3 the latter condition occurs up to $f_{VB} = 0.45$, which is near the f_{VB} value where σ ceases to have a positive second derivative. This is hence experimental evidence that a CC "threshold" has been crossed, although it may not be a sharp threshold. The negative second derivative of σ versus f_{VB} starting at about 0.8 likely signals the decrease in copolyelectrolyte specific conductivity as ξ falls toward zero, while the copolyelectrolytes chain mass remains approximately constant. Increase in reactor viscosity negligibly affected σ in this experiment, although it may play a role in more concentrated reactions.

Not all starting ratios of [VB]/[Aam] led to blends of copolyelectrolyte and neutral homopolymer, polyacrylamide (PAM). Figure 4 contrasts the cases of 10/90, 25/75, 50/50, and 75/25 (%). For the first case, already seen above, and the second, the two phase conversion of Aam results, whereas in the latter two cases, there is only a single phase of conversion for both Aam. The inset shows that VB has a single phase of conversion in each experiment, but in the latter cases it is not exhausted, and continues to co-convert with Aam throughout the reaction; i.e. no blend is produced. The two-phase acrylamide conversion

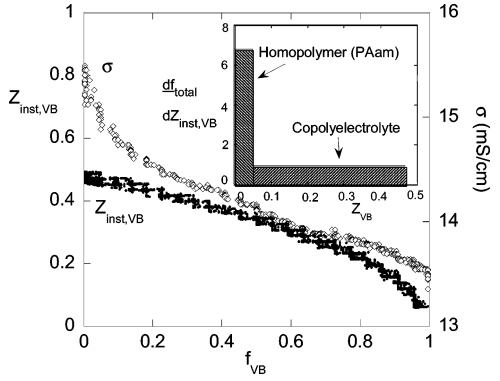

Figure 3. Composition drift during polymerization, $Z_{inst,VB}$ vs f_{VB}, and evolution of σ vs f_{VB}. Inset shows average composition distribution.

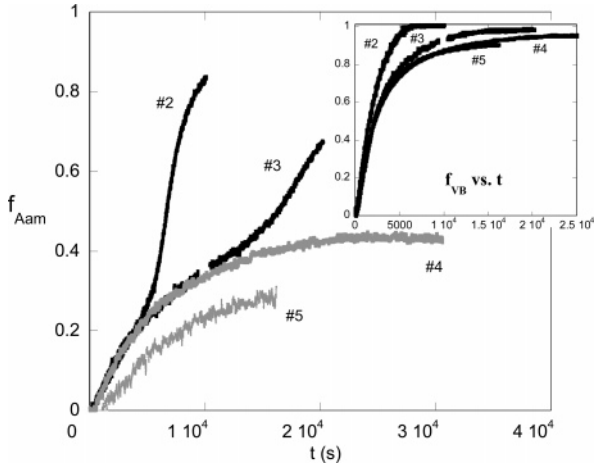

Figure 4. Conversion of Aam for several different starting ratios of [VB]/[Aam], in 0.100M NaCl. Bimodality is lost between VB/Aam 25/75 and 50/50.

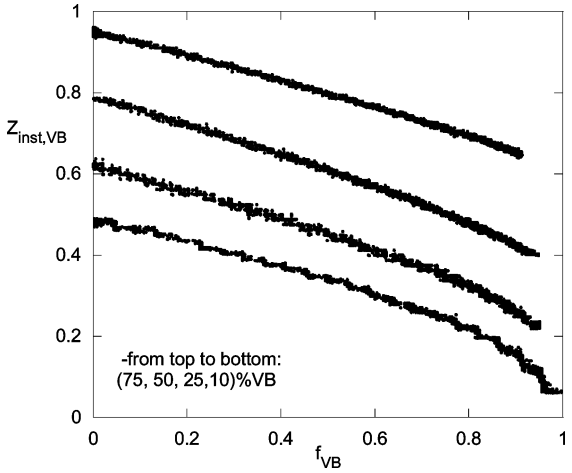

Figure 5. Composition drift of VB vs f_{VB} for several different starting ratios of VB/Aam.

was also found in the cases of 1.5/98.5, 5/95, and 10/90 (%) VB/AaM copolymerization reactions carried out in water with no added salt in the reactor.

Figure 5 shows $Z_{inst,VB}$ for the different starting values of VB/Aam. From the naïve CC point of view, only the lowest value, 10/90, leads to a $Z_{inst,VB}$ that significantly crosses the putative CC threshold (at $Z_{inst,VB} = 0.35$), and 25% has only a small portion that crosses it. Hence, in the other cases it would be surmised that the ξ distribution is essentially "monodisperse", that is, $\xi \sim 1$ along the chains.

It is emphasized that all the data presented here are model-independent, including the striking two-phase copolymerization kinetics. Traditionally, different models for reactivity ratios (RR) have been used to interpret kinetics and composition distributions. In fact, an extended numerical error in variable method[52] was developed to obtain RR from ACOMP and applied to methyl methacrylate/styrene copolymerization.[43] The authors are separately analyzing the current data, with tentative values of $r_{Aam} \approx 0.18$, $r_{NaSS} \approx 2.0$ in 0.100M NaCl. There is also strong evidence of implicit penultimate effects[47,48] on the kinetics of the VB/Aam system. It is not known at this time whether the RR, with or without implicit penultimate effects will explain the two phase kinetics, nor if any effects such as possible micellization of VB monomers, or crossing the overlap concentration during polymerization may effect the behavior.

Other recent methods for continuously monitoring copolymerization reactions that allowed the reactivity ratios to be computed from online data were applied by several groups,[53−55] including for terpolymerization reactions.[56]

End-Product Characterization by ACM. *Light Scattering.* The trivariate distribution produced during copolyelectrolyte synthesis should control end-product solution behavior. Light scattering at low to moderate IS can be dominated by second and third virial coefficients A_2 and A_3, respectively. Extensive theories for A_3 have been developed for monodisperse chain polymers.[57,58] A theoretical quantity of interest is

$$g = \frac{A_3}{MA_2^2} \tag{3}$$

For hard spheres $g = 5/8$, whereas for coil polymers, measured values typically range from 0.15 to 0.56.[59−61] This range of values has typically been found in low to moderate polydispersity polymers. Monte Carlo simulations yielded a "universal" asymptotic value at large M of 0.30.[62] Nearly constant values of g for linear sodium hyaluronate was found over a wide range of IS.[63] Stockmayer and Casassa[52] pointed out early on that in polydisperse (including bimodal) solutions the values of A_2 and A_3 measured by light scattering are not the same as those found in the usual expansion for osmotic pressure, so that caution must be used when comparing these quantities.

For the bimodal end-products the ACM results lead quickly to the frontier of both experimental and theoretical knowledge.[64] Experiments show that definitive theories for cross-species interactions are quite incomplete, even for simple mixtures of two monodisperse, neutral polymers of the same species but different mass (e.g., polystyrene in toluene).[65]

Multicomponent scattering formalisms can be invoked for the case of multiple interacting polymer species.[66,67] One approach for a system of two distinct polymers a and b gives

$$I_{total} = S_{aa}(q)P_a(q)K_a c_a M_a + 2S_{ab}(q)[P_a(q)K_a c_a M_a P_b(q)K_b c_b M_b]^{1/2} + S_{bb}(q)P_b(q)K_b c_b M_b \tag{4}$$

for which there are theories to model intraparticle form factor $P(q)$, and interparticle structure factors $S_{ab}(q)$.[59,68] I_{total} is the excess Rayleigh scattering ratio (cm^{-1}), and K for each species is the usual optical constant, which for vertically polarized incident light is $K = 4\pi^2 n^2 (dn/dc)^2 / N_A \lambda^4$.

Figure 6 shows $Kc/I(q = 0)$ versus polymer concentration at different IS, from ACM for the copolyelectrolyte/neutral polymer blend produced at 0.100M NaCl. I is the Rayleigh scattering ratio (in cm^{-1}). At $q = 0$, $P(q) = 1$ for each

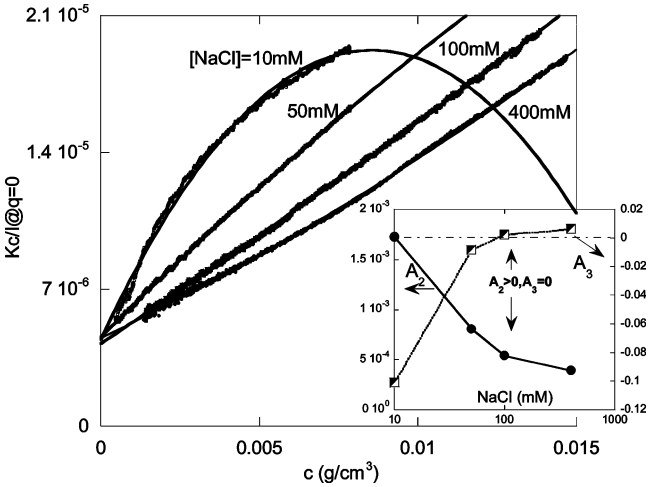

Figure 6. $Kc/I(q = 0)$ vs polymer concentration c, at different IS for the end-product of the 10/90 experiment. Inset shows A_2 and A_3 vs IS.

component, leaving $S_{aa}(0)$, $S_{ab}(0)$, and $S_{bb}(0)$ to incorporate the effects of A_2, A_3, and higher terms.

In order to gain some qualitative insight, effective light-scattering A_2 and A_3 values are computed from the Figure 6 data using the conglomerate homopolymer expression

$$\frac{Kc}{I(c,0)} = \frac{1}{M_w} + 2A_2c + 3A_3c^2 + O(c^3) \qquad (5)$$

A_2 is positive and decreases versus IS (inset), as is usually found, whereas A_3 is negative at low IS, passes through zero around 0.100 M, and is positive at higher IS. For the homopolymers (PVB and PAM), A_2 and A_3 are positive under all IS conditions. In fact, for purely repulsive interparticle potentials, e.g., hard spheres, A_2 and A_3 will be positive even for multimodal populations.[69] Positive values of third virial coefficients were recently reported for mixtures of proteins and chain molecules with a weak attraction between the two species.[70]

Since A_2 and A_3 involve integrating interparticle correlation functions, and hence potentials, over all space, they simply give a net result of what may include both repulsive and attractive regions of potential. The negative A_3 may reflect attractive components; e.g., one may surmise a polyion interaction with the dipole moment of neutral PAM, based on an attractive force due to the inhomogeneous electric field around the copolyelectrolyte, $\vec{F} = -\nabla U = \vec{p}\cdot\nabla\vec{E}$. Such an interaction would be progressively screened with salt, leaving only the steric repulsion potential at high IS. It is noted that just because $A_2 = 0$ at the Θ-point, a finite value of A_3 is not precluded.[71,72]

Strong evidence that this behavior is due to the bimodality of the end-product is seen in Figure 7, which shows ACM data, $Kc/I(q = 0)$ vesus c, at 0.010 M NaCl for different end-products. The data indicate that the scattering behavior is linked to the cross-terms between the copolyelectrolytes and the neutral PAM populations: A_3 is negative for 10% and 25% VB, and ACOMP revealed bimodal end-products for these starting compositions (Figure 4), whereas the other compositions, yielding unimodal end-products, giving the usual, positive A_3. The inset to Figure 6 shows the trends in A_2 and A_3.

To explore this idea further, ACM experiments were made on deliberate mixtures of polymers. Figure 7 shows some of these results. Indeed, it is exclusively due to the mixtures that A_3 ever becomes negative. As seen, A_3 is positive and large for PVB and positive and small for PAM, but becomes negative for the mixtures of PVB and PAM measured. In subsequent

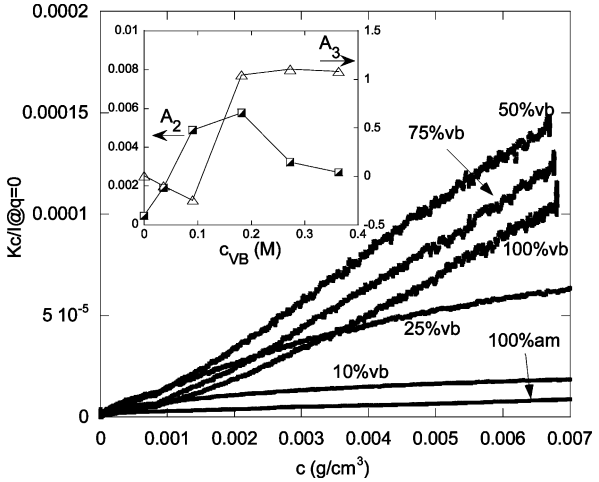

Figure 7. $Kc/I(q = 0)$ vs c for the end-products of the experiments in Table 1, at $C_s = 0.010$ M. The inset shows A_2 and A_3 vs starting composition of the reaction.

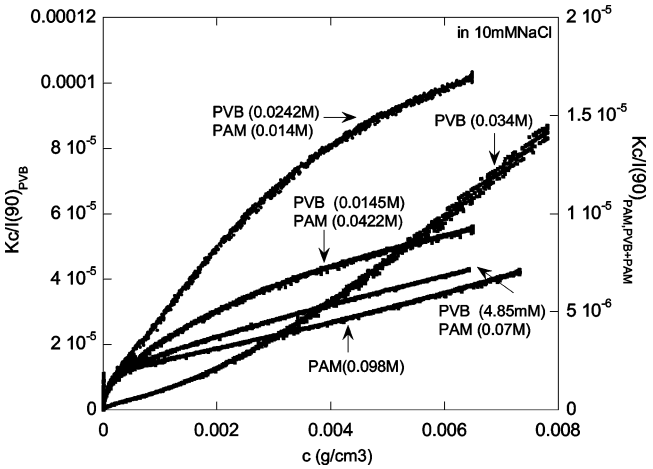

Figure 8. $Kc/I(\theta = 90°)$ for mixtures of PVB and PAM.

experiments it was found that sodium hyaluronate mixed with PAM gives the same A_2 and A_3 trend as the VB/Aam case.

It is beyond the scope of this work to find a theoretical resolution of the observed behavior of equivalent A_3 for mixtures of polyelectrolytes and neutral polymers. The combined ACOMP and ACM methods, however, provide an experimental means for exploring this complex issue.

Reduced Viscosity. In contrast to the light scattering data, the reduced viscosity, η_r data present no unusual behavior. Figure 8 shows η_r versus c at IS = 0.010 M for the end-products from the Table 1 reactions. These all yield the usual linear behavior, with very small slopes over the range of measurement. The slope measures the intermolecular hydrodynamic interactions and there are no qualitative changes between bimodal and unimodal end-products. The variations in the $c = 0$ intercept, which equals $[\eta]_w$, are due both to the molar mass differences of the samples, and their ξ distributions.

This behavior is rationalized as follows: Intramolecular electrostatic interactions can strongly affect the dimensions of polyelectrolytes, and hence their $[\eta]_w$, but purely electrostatic interactions between polymers have little effect on how they hydrodynamically perturb the fluid velocity flow field around each other, and hence do not create large interparticle effects at the low concentrations used here. Light scattering is much more sensitive to "soft" interpolymer interactions, such as the electrostatic interaction, since the virial coefficients integrate whatever interparticle potentials exist over all spatial separations

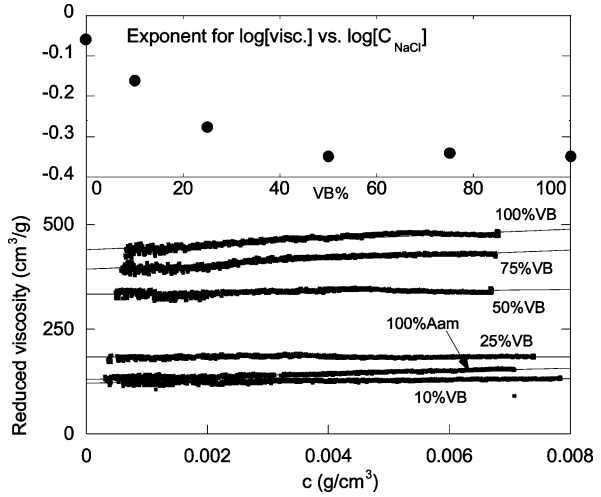

Figure 9. η_r vs c at IS = 0.010 M for different end-products. Top frame shows the exponent b, in the pseudoscaling law $\log(\eta_r)$ vs log(IS).

between pairs of particles. Hence, the changes in light scattering behavior due to interactions is much more striking than those for viscosity.

$[\eta]_w$ has interesting behavior versus IS. For each end-product $[\eta]_w$ was determined at IS = 0.010, 0.100, and 0.300 M. While no simple power law is expected to relate $[\eta]_w$ versus IS, using these three points and fitting a pseudo-power law of the form $[\eta]_w \approx aIS^b$ yields the exponents for b as a rough and ready indicator of how the end-product $[\eta]_w$ reacts to IS. The values of b are shown in the Figure 8 inset. For PAM b is close to zero, as expected, and b levels out at 0.35 for VB% $\geq$ 50%; i.e., this is consistent with the notion that for a high % of VB in the chains, CC will limit ξ to $\approx$ 1, so that there will be no difference in the ξ distribution above this threshold. This theoretical conclusion is supported by the Figure 8 inset. If the higher percentage VB end-products had higher ξ, then b would continue to decrease with ξ, instead of leveling off.

Summary

It has been demonstrated that ACOMP can be used to follow the evolution of the average bivariate composition/molar mass distribution during synthesis of copolyelectrolytes, and that under relatively low starting percentages of VB bimodal end-products are produced, which are blends of copolyelectrolyte and neutral homopolymer (PAM). The conductivity monitoring shows a strong correlation between its decrease and incorporation of VB, and it ceases to change once VB is fully consumed in the bimodal reactions. The relationship between conductivity changes with conversion and the evolution of the ξ distribution are complex, involve many factors, and are beyond the scope of this initial study.

The end-product characterization using ACM shows dramatically different behavior between those end-products that are bimodal and those that are not. In the former case A_3 is actually negative at low IS, whereas A_2 is always positive for all end-products at all IS. The negative A_3 is surmised to be related to an attractive ion-dipole interaction between the neutral polymer and the copolyelectrolyte in the bimodal populations. This interaction is screened away at high IS leaving A_3 positive. Experimental proof that this behavior is due to interactions between the bimodal populations is yielded by using deliberate blends of neutral polymer and copolyelectrolyte, where it was possible to again obtain negative A_3 at low IS. The reduced viscosity behavior is entirely insensitive to these soft interchain interactions, and no striking differences are found between unimodal and bimodal end-products. On the other hand, the relationship between $[\eta]_w$ and IS for the different end-products supports the notion that counterion condensation limits the linear charge density for copolyelectrolytes with high levels of VB.

It is hoped that this approach will lead to better theoretical understanding of the kinetics of copolyelectrolyte synthesis, polyelectrolyte properties, especially scattering behavior, and provide a practical means of controlling the distributions to produce polyelectrolytes of desired properties.

Acknowledgment. Support from NSF CBET 0623531, NASA NCC3-946 and La. BoR RD-B-7 is acknowledged. A. Paril acknowledges support from TUBITAK-BDP during his visit to Tulane.

References and Notes

(1) McKenna, T. F.; Fevotte, G.; Graillat, C.; Guillot, J. *Chem. Eng. Res. Des.* **1996**, *74*, A3, 340−348.
(2) Sauzedde, F.; Hunkeler, D. *Int. J. Polym. Anal. Charact.* **2001**, *6*, 295−314.
(3) Wild, L. *Adv. Polym. Sci.* **1991**, *98*, 1−47.
(4) Anantawaraskul, S.; Soares, J. B. P.; Wood-Adams, P. *J. Polym. Sci. B: Polym. Phys.* **2003**, *41*, 1762−1778.
(5) Feng, Y.; Hay, J. N. *Polymer* **1998**, *39*, 6723−6731.
(6) Zacur, R.; Goizueta, G.; Capiati, N. *Polym. Sci. Eng.* **2000**, *40*, 8, 1921−1930.
(7) Anantawaraskul, S.; Soares, J.; Wood-Adams, P. M. *Macromol. Chem. Phys.* **2004**, *205*, 771−777.
(8) Meehan, E.; O'Donohue, S. *Adv. Chem. Ser.* **1995**, *247*, 243−251.
(9) Netopilik, M.; Bohdanecky, M.; Kratochvil, P. *Macromolecules* **1996**, *29*, 18, 6023−6030.
(10) Kramer, I.; Pasch, H.; Handel, H. A. *Macromol. Chem. Phys.* **1999**, *200*, 1734−1744.
(11) Montaudo, M. S. NMR Spectroscopy of Polymers in Solution and in the Solid State. *ACS Symp. Ser.* **2003**, *834*, 358−381.
(12) Tacx, J. C. J. F.; German, A. L. *Polymer* **1989**, *30*, 918−927.
(13) Mori, S. *Anal. Chem.* **1988**, *60*, 1125−1128.
(14) Philipsen, J. A. H. *J. Chromatography* **2004**, *1037*, 329−350.
(15) Nierlich, M.; Williams, C. E.; Boue, F.; Cotton, J. P.; Daoud, M.; Farnoux, B.; Jannink, G.; Picot, C.; Moan, M.; Wolff, C.; Rinaudo, M.; de Gennes, P. G. *J. Phys. (Paris*) **1979**, *40*, 701−704.
(16) Nallet, F.; Jannink, G.; Hayter, J.; Oberthur, R.; Picot, C. *J. Phys. (Paris*) **1983**, *44*, 87−99.
(17) Maier, E. E.; Krause, R.; Deggelmann, M.; Hagenbuechle, M.; Weber, R.; Fraden, S. *Macromolecules* **1992**, *25*, 1125−1133.
(18) Wang, L.; Bloomfield, V. A. *Macromolecules* 1**991**, *24*, 5791−5795.
(19) Drifford, M.; Dalbiez, J. P. *J. Phys. Chem.* **1984**, *88*, 5368−5375.
(20) Li, X.; Reed, W. F. *J. Chem. Phys.* **1991**, *94*, 4568−4580.
(21) Forster, S.; Schmidt, M.; Antonietti, M. *Polymer* **1990**, *31*, 781−792.
(22) Morfin, I.; Reed, W. F.; Rinaudo, M.; Borsali, R. *J. Phys. (Paris*) **1994**, *4*, 1001−1019.
(23) Reed, W. F. *J. Chem. Phys.* **1994**, *100*, 7825−7827.
(24) Odijk, T. *J. Polym. Sci., Phys. Ed.* **1977**, *15*, 477−483.
(25) Skolnick, J.; Fixman, M. *Macromolecules* **1977**, *10*, 9444−9448.
(26) Odijk, T.; Houwaart, A. C. *J. Polym. Sci., Phys. Ed.* **1978**, *16*, 627−639.
(27) Beer, M.; Schmidt, M.; Muthukumar, M. *Macromolecules* **1997**, *30*, 8375−8385.
(28) Meullenet, J. P.; Schmitt, A.; Drifford, M. *J. Phys. Chem.* **1979**, *83*, 1924−1927.
(29) Klein, J. W.; Ware, B. R. *J. Chem. Phys.* **1984**, *80*, 1334−1339.
(30) Welch, C. F.; Hoagland, D. A. *Langmuir* **2003**, *19*, 1082−1088.
(31) Starkweather, M. E.; Hoagland, D. A.; Muthukumar, M. *Macromolecules* **2000**, *33*, 1245−1253.
(32) Manning, G. S. *J. Chem. Phys.* **1969**, *51*, 934−938.
(33) Oosawa, F. *Polyelectrolytes*; Marcel Dekker: New York, 1971.
(34) Deserno, M.; Holm, C.; May, S. *Macromolecules* **2000**, *33*, 199−206.
(35) Chu, J. C.; Mak, C. H. *J. Chem. Phys.* **1999**, *110*, 2669−2679.
(36) Wilson, R. W.; Bloomfield, V. A. *Biochemistry* **1979**, *18*, 2192−2196.
(37) Hinderberger, D.; Spiess, H. W.; Jeschke, G. *J. Phys. Chem. B* **2004**, *108*, 3698−3704.
(38) Muthukumar, M. *J. Chem. Phys.* **2004**, *120*, 9343−9350.

(39) Rouzina, I.; Bloomfield, V. A. *J. Phys. Chem.* **1996**, *100*, 9977−9989.
(40) Rouzina, I.; Bloomfield, V. A. *J. Phys. Chem.* **1996**, *100*, 4292−4304.
(41) Florenzano, F. H.; Strelitzki, R.; Reed, W. F. *Macromolecules* **1998**, *31*, 7226−7238.
(42) Mignard, E.; Leblanc, T.; Bertin, D.; Guerret, O.; Reed, W. F. *Macromolecules* **2004**, *37*, 966−975.
(43) Çatalgil-Giz, H.; Giz, A.; Alb, A. M.; Oncul, A. K.; Reed, W. F. *Macromolecules* **2002**, *35*, 6557−6571.
(44) Elizalde, O.; Asua, J. M.; Leiza, J. R. *App. Spectrosc.* **2005**, *59*, 1280−1285.
(45) Reis, M. M.; Araujo, P. H. H.; Sayer, C.; Giudici, R. *J. App. Polym. Sci.* **2004**, *93*, 1136−1144.
(46) Vrij, A.; Overbeek, J. Th. G. *J. Colloid Sci.* **1962**, *17*, 570−582.
(47) Casassa, E. F.; Eisenberg, H. *J. Phys. Chem.* **1960**, *64*, 753−762.
(48) Ooi, T. *J. Polym. Sci.* **1958**, *28*, 459−466.
(49) Farinato, R. Personal communication, 2001.
(50) Sorci, G. A.; Reed, W. F. *Langmuir* **2002**, *18*, 353−364.
(51) Reed, W. F. *Macromolecules* **2000**, *33*, 7165−7172.
(52) Sunbul, D.; Çatalgil-Giz, H.; Reed, W. F.; Giz, A. *Macromol. Theory Simul.* **2004**, *13*, 162−168.
(53) Shaikh, S.; Chattopadhyay, S.; Puskas, J. E. *Abstr. Pap. − Am. Chem. Soc.* **2002**, *223*, 322.
(54) van den Brink, M.; Pepers, M.; van Herk, A. M.; German, A. L. *Polym. React. Eng.* **2001**, *9*, 101.
(55) Hua, H.; Dubé, M. A. *Polym. React. Eng.* **2002**, *10*, 21.
(56) Othman, N.; Fevotte, G.; McKenna, T. F. *Polym. React. Eng.* **2001**, *9*, 271.
(57) Stockmayer, W. H.; Casassa, E. F. *J. Chem. Phys.* **1952**, *20*, 1560−1566.
(58) Koyama, R. *J. Chem. Phys.* **1957**, *27*, 234−239.
(59) Kniewske, R.; Kulicke, W. M. *Makromol. Chem.* **1985**, *18*, 201−209.
(60) Nakamura, Y.; Norisuye, T.; Teramaoto, A. *J. Polym. Sci., Polym. Phys. Ed.* **1991**, *29*, 153−159.
(61) Oettinger, H. C. *Macromolecules* **1985**, *18*, 93−98.
(62) Bruns, W. *Macromolecules* **1997**, *30*, 4429−4431.
(63) Sorci, G. A.; Reed, W. F. *Macromolecules* **2002**, *35*, 5218−5227.
(64) Berry, G. C., Total Intensity Light Scattering from Solutions of Macromolecules. In *Soft Matter: Scattering, Manipulation & Imaging*; Pecora, R., Borsali, R., Eds.; in Press.
(65) Sato, T.; Norisuye, T.; Fujita, H. *J. Polym. Sci., Part B: Polym. Phys.* **1987**, *25*, 1−17.
(66) Benmouna, M.; Vilgis, T.; Hakem, F.; Negadi, A. *Macromolecules* **1991**, *24*, 6418−6425.
(67) Higgins, J. S.; Benoit, H. C. *Polymers and Neutron Scattering*; Clarendon Press: Oxford, 1994; pp 119−120.
(68) de Gennes, P. G. *Scaling Concepts in Polymer Physics*; Cornell University Press: Ithaca, NY, 1979.
(69) Lebowitz, J. L. *Phys. Rev.* **1964**, *133*, A895−904.
(70) Bloustine, J.; Virmani, T.; Thurston, G. M.; Fraden, S. *Phys. Rev. Lett.* **2006**, *96*, 087803-1−087803-4.
(71) Yamakawa, H. *J. Chem. Phys.* **1965**, *42*, 1764−1771.
(72) Mizuno, T.; Terao, K.; Nakamura, Y.; Norisuye, T. *Macromolecules* **2005**, *38*, 4432−4437.